HHS Public Access

Author manuscript

Oncogene. Author manuscript; available in PMC 2017 March 10.

Published in final edited form as:

Oncogene. 2017 March ; 36(10): 1394–1403. doi:10.1038/onc.2016.305.

Silencing Vimentin Expression Decreases Pulmonary Metastases in a Pre-Diabetic Mouse Model of Mammary Tumor Progression

Zara Zelenko[1], **Emily J. Gallagher**[1], **Aviva Tobin-Hess**[1], **Valentina Belardi**[1], **Ran Rostoker**[2], **Jeffery Blank**[1], **Yemisi Dina**[1], and **Derek LeRoith**[1,2]

[1]Division of Endocrinology, Diabetes and Bone Diseases, Icahn School of Medicine at Mount Sinai, One Gustave L. Levy Place, Box 1055, New York City, New York, 10029, USA

[2]Clinical Research Institute at Rambam (CRIR) and the Faculty of Medicine, Technion, Diabetes and Metabolism Clinical Research Center of Excellence, Efron St, Haifa, 33705, Israel

Abstract

Increased breast cancer risk and mortality has been associated with obesity and Type 2 diabetes (T2D). Hyperinsulinemia, a key factor in obesity, pre-diabetes and T2D, has been associated with decreased breast cancer survival. In the current study, a mouse model of pre-diabetes (MKR mouse) was used to investigate the mechanisms through which endogenous hyperinsulinemia promotes mammary tumor metastases. The MKR mice developed larger primary tumors and greater number of pulmonary metastases compared to wild type (WT) mice after injection with c-Myc/Vegf overexpressing MVT-1 cells. Analysis of the primary tumors showed significant increase in Vimentin protein expression in the MKR mice compared to WT. We hypothesized that Vimentin was an important mediator in the effect of hyperinsulinemia on breast cancer metastasis. Lentiviral shRNA knockdown of Vimentin led to a significant decrease in invasion of the MVT-1 cells and abrogated the increase in cell invasion in response to insulin. In the pre-diabetic MKR mouse, Vimentin knockdown led to a decrease in pulmonary metastases. *In vitro*, we found that insulin increased pAKT, prevented Caspase 3 activation, and increased Vimentin. Inhibiting the PI3K/AKT pathway, using NVP-BKM120, increased active Caspase 3 and decreased Vimentin levels. This study is the first to show that Vimentin plays an important role in tumor metastasis *in vivo* in the setting of pre-diabetes and endogenous hyperinsulinemia. Vimentin targeting may be an important therapeutic strategy to reduce metastases in patients with obesity, pre-diabetes or T2D.

Keywords

Type 2 Diabetes; Breast Cancer; Hyperinsulinemia; Vimentin; Metastases

Corresponding Author: Derek LeRoith, Division of Endocrinology, Diabetes and Bone Diseases, Icahn School of Medicine at Mount Sinai, One Gustave L. Levy Place, Box 1055, New York, NY 10029, Tel: 212-241-6306, Fax: 212-241-4159, Derek.LeRoith@mssm.edu.

Conflict of Interest:
The authors disclose no potential conflicts of interest.

Introduction

Epidemiological studies have shown that obesity and Type 2 Diabetes (T2D) prevalence has grown significantly over the past decade. In breast cancer patients, those with T2D have a significantly increased mortality rate compared with women without T2D (1). There are a number of potential factors common to T2D, obesity and the metabolic syndrome that can lead to increased tumor growth in the setting of T2D, such as insulin resistance, hyperinsulinemia, insulin-like growth factor-1 (IGF-1), hyperglycemia, dyslipidemia, inflammatory cytokines and adipokines (1–5). Of these factors, hyperinsulinemia has emerged to be a key player and has been associated with decreased breast cancer survival and recurrence free survival (6, 7). In obesity and T2D, insulin resistance develops in metabolic tissues, then due to beta cell compensation, hyperinsulinemia occurs. (8, 9). Insulin resistance and hyperinsulinemia are present for many years prior to the development of hyperglycemia in individuals who develop T2D...

The MKR mice were generated by the LeRoith group by overexpressing the kinase dead IGF-1R, under control of the muscle creatine kinase promoter (10). The female MKR mice show significant insulin resistance and hyperinsulinemia, representing a pre-diabetic state (11). These mice have increased tumor growth following carcinogen, transgenic or orthotopic induction of mammary tumors (11, 12). We aim to investigate the mechanisms whereby hyperinsulinemia drives breast cancer metastases, as mortality from breast cancer occurs from metastatic disease.

In the current study, we provide evidence that hyperinsulinemia increases the protein expression of Vimentin. Vimentin, a 57 kDa protein, is a type III intermediate filament, expressed in cells of mesenchymal origin (13). It is typically considered to be an epithelial-mesenchymal transition (EMT) marker (14). It has been shown that an increase in Vimentin expression is associated with greater invasion of metastatic cell lines *in vitro* (15, 16). In this study we show that primary tumors of the pre-diabetic MKR mice had significantly increased Vimentin protein expression, which we hypothesized to be due to endogenous hyperinsulinemia. We found that insulin increases Vimentin protein expression *in vitro*, which is inhibited with a PI3K inhibitor. We found that knockdown of Vimentin expression leads to decreased cell invasion, and less numerous pulmonary metastases in the hyperinsulinemic mice. The results of this study suggest pre-diabetes and hyperinsulinemia are associated with more advanced breast cancer, due to upregulation of Vimentin, and that inhibiting Vimentin upregulation may reduce metastases in breast cancer patients with obesity, diabetes and the metabolic syndrome.

Results

Tumors from pre-diabetic mice have increased Vimentin protein expression

The hyperinsulinemic, pre-diabetic female homozygous MKR (MKR) mice have been previously described (11, 17). We injected 100,000 MVT-1 cells into the 4th mammary fat pad of 8 week old control (WT) and MKR mice. There was a significant increase in tumor size in MKR mice when compared to the tumors from the WT mice (Figure 1A), consistent

with our previous studies (12). We also observed significant increase in average surface pulmonary metastasis per mouse in the MKR mice compared to WT mice (Figure 1B). The primary tumors from WT and MKR mice were flash frozen and protein was extracted. In order to determine whether the increase in metastases in the MKR mice was due to an increase in EMT in the primary tumors, we analyzed EMT markers including, E-cadherin, N-cadherin, Vimentin, Twist and Snail. No significant changes in protein or gene expression levels of Twist, Snail, Zeb1 and E-cadherin were seen *in vivo* (Figure S1). There was an increase in Vimentin protein expression in the tumors from the MKR mice compared to WT (Figure 1C). As two bands were consistently observed on the Western blot, Vimentin was immunoprecipitated from the protein lysate and was analyzed by LC-MS. Proteomic analysis revealed that both of the bands seen on the western blot are Vimentin. The higher molecular weight band contains threonine 417 and serine 420 phosphorylation sites not found in the lower molecular weight band (Figure S2).

Immunofluorescent staining of formalin fixed, paraffin embedded (FFPE) tumors from the WT and MKR mice confirmed the increase of Vimentin expression in tumors from MKR mice compared to WT mice (Figure 2A, B). In order to examine if the cells that expressed Vimentin were the MVT-1 tumor cells or invading fibroblasts, MVT-1 cells were GFP tagged and injected orthotopically into the 4^{th} mammary fat pad of WT and MKR mice, as previously described (18). Immunofluorescent staining of FFPE tumors showed that the GFP positive cells also stained for Vimentin, demonstrating that the increase in Vimentin is from the primary tumor cells and not from invading fibroblasts (Figure 2C).

MVT-1 cells with Vimentin knockdown demonstrate a normal insulin-mediated signaling response

In order to determine whether insulin was capable of driving the increase in Vimentin protein expression in the MVT-1 cells were stimulated with 10nM of insulin for 48hours. We observed a significant increase in Vimentin protein expression following the insulin stimulation (Figure 3A). No changes in other EMT markers were observed after insulin stimulation (Figure S3). Moreover, we found that insulin significantly increased Vimentin protein expression *in vitro* in the mouse MET-1 Cells (derived from MMTV-PyVmT/FVB-N transgenic mice (19)) (Figure S4).

In order to determine the importance of Vimentin facilitating the increase in insulin-mediated tumor metastases, MVT-1 cells were transduced with lentiviral plasmid DNA with Control shRNA sequence or Vimentin shRNA sequences. After stable transduction was achieved with puromycin selection, the cells were analyzed for the degree of Vimentin knockdown. The Vimentin protein from the Control shRNA showed no difference when compared to the parental non-transduced MVT-1 cell line (Figure 3B). Two Vimentin clones showed significant decrease in Vimentin protein expression. We observed a 60% knockdown of Vimentin protein expression in clone Vimentin-317673 and a 77% knockdown of Vimentin protein expression in clone Vimentin-317676 (Figure 3B). Quantitative Real Time PCR analysis showed a 60% and a 90% decrease in Vimentin gene expression in the clones Vimentin-317673 and Vimentin-317676, respectively (Figure 3C). The MVT-1 control and Vimentin knockdown cells were analyzed for invasion in Complete Medium. There was a

significant decrease in the invasion capacity of both of the MVT-1 Vimentin knockdown clones (Figure 3D). The Vimentin-317676 clone showed greater decrease in invasion compared to the Vimentin-317673 clone. The clone with the greater knockdown of both Vimentin gene and protein expression (Vim-317676) was used for future *in vivo* and *in vitro* studies.

As Vimentin has been reported to be involved in signal transduction (20, 21), we next determined if silencing Vimentin affected the insulin-signaling pathway. The MVT-1 control and MVT-1 Vimentin knockdown cells were stimulated with 10nM insulin for 15min. Following the insulin stimulation we observed an increase in AKT phosphorylation in both the MVT-1 control and MVT-1 Vimentin knockdown cells (Figure 4A, B). This indicated that the Vimentin knockdown did not alter the insulin-mediated activation of the PI3K/AKT pathway.

Lentiviral knockdown of Vimentin in MVT-1 cells leads to a decrease in cell invasion in response to insulin

The MVT-1 control and Vimentin knockdown cells were analyzed for proliferation, migration and invasion. There was no difference in OD calculated cell number between the MVT-1 control and MVT-1 Vimentin knockdown cells at each time point (Figure 5A). There was no difference in the MVT-1 control or Vimentin knockdown migration capacity through an 8μm pore (Figure 5B). Stimulation with insulin led to an increase in invasion of MVT-1 control cells, but did not significantly increase the invasion of MVT-1 Vimentin knockdown cells (Figure 5C). Our data demonstrate that Vimentin is important for mediating insulin's effect on cell invasion.

Knockdown of Vimentin in MVT-1 tumors leads to decreased number of pulmonary metastases in the hyperinsulinemic MKR mice

In order to study the effects of knocking down Vimentin on tumor growth and lung metastases in the mouse model of pre-diabetes, WT and MKR mice were split into 4 groups and orthotopically injected with 100,000 MVT-1 control cells (8–10 mice per group) and 100,000 MVT-1 Vimentin knockdown cells (10–13 mice per group). The four groups were the WT Control (Ctrl), WT Vimentin knockdown (VimKD), MKR Ctrl, and MKR VimKD. A significant increase in primary tumor size was found in the MKR Ctrl mice compared with the WT Ctrl mice (Figure 6A). However, no significant difference was observed between the tumor volume of the Vimentin knockdown and control tumors in MKR or WT mice (Figure 6A).

We observed significant increase in average number of surface pulmonary metastases per mouse from the MVT-1 control tumors in the MKR group compared to WT group (Figure 6B, Figure S5) consistent with our results in the parental, non-transduced cells (Figure 1A). There was a significant decrease in surface pulmonary metastases in the MKR VimKD group compared to the MKR Ctrl group (Figure 6B, Figure S5). There was a significant decrease in the sizes of pulmonary metastases in the MKR VimKD group compared to the MKR Ctrl group (Figure S5).

Analyzing the protein lysates from the primary tumors of the four groups, we observed an increase in Vimentin protein expression in the MKR Ctrl group compared to the WT Ctrl group (Figure 6C). We also confirmed that the primary tumors of the MVT-1 Vimentin knockdown cells, showed a significant decrease in Vimentin protein expression at the end of the *in vivo* study (Figure 6C).

Therefore down-regulating Vimentin protein expression in primary tumors led to no change in primary tumor size, but a significant reduction in pulmonary metastases in the pre-diabetic, hyperinsulinemic MKR mice.

Insulin leads to the increase of Vimentin expression by activating PI3K/AKT signaling and preventing Caspase activation

In order to understand how hyperinsulinemia could promote the increase of Vimentin expression, we hypothesized that the PI3K/AKT signaling pathway may be a mediator, as we have found this pathway to be activated in MVT-1 tumors from MKR mice, and *in vitro* by insulin (12). MVT-1 parental cells were stimulated with NVP-BKM120, a known PI3K inhibitor. As previously described, an increase in Vimentin protein expression after 48h stimulation with 10nM Insulin was observed (Figure 7A, B). Using 500nM of the NVP-BKM120 inhibitor, a decrease of total Vimentin expression was observed compared to vehicle control (Figure 7A, B). Furthermore, NVP-BKM120 prevented the increase in Vimentin expression in response to insulin (Figure 7A, B). Examining the PI3K/AKT pathway, we observed that insulin-mediated phosphorylation of AKT(Ser473) was effectively inhibited following NVP-BKM120 stimulation (Figure 7C, D).

In soft tissue sarcoma cells, AKT activation has been found to prevent Caspase-mediated Vimentin proteolysis (21). Therefore, we examined if the effect of insulin and NVP-BKM120 on Caspase 3 cleavage. Insulin decreased the amount of active Caspase 3 and PI3K inhibition by NVP-BKM120 promoted an increase in active Caspase 3 (Figure 8A, B). We saw a similar decrease in the activation of Caspase 3 by insulin in the MET-1 cells (Figure S4). There was also an increase in the cleavage of carboxy-terminal catalytic domain of poly(ADP-ribose) polymerase-1 (PARP), a target of Caspases (22) (Figure 8C, D). There was a significant decrease in full length PARP following NVP-BKM120 stimulation in the MVT-1 cells (Figure 8C).

Discussion

T2D, obesity and the metabolic syndrome have been associated with an increase incidence of breast cancer and increased mortality from breast cancer. (23–27). Insulin resistance and hyperinsulinemia are common in obesity, and characterize pre-diabetes and early T2D. Studies have shown that hyperinsulinemia is associated with decreased breast cancer survival and recurrence free survival (6, 7). Pre-clinical studies support the role of hyperinsulinemia in promoting breast cancer progression (11, 12). In this study, we utilized a hyperinsulinemic mouse model to investigate key factors affecting the significant increase in pulmonary metastases observed in the setting of hyperinsulinemia. We found that Vimentin protein expression was significantly increased in the primary tumors from the hyperinsulinemic MKR mice compared to the WT controls. Vimentin has classically been

regarded as a marker for cells undergoing EMT. However, it may play an important role in the motility of mesenchymal cells and metastatic tumors (15, 28). Outside of the setting of hyperinsulinemia, increased Vimentin expression has been seen in various cancers, including breast, prostate and lung cancers (29). This increase has been associated with increased tumor growth, tumor invasion and poor prognosis (16, 29).

Previous studies have established a link between IGF-1 signaling and Vimentin, where IGF-1 stimulation led to Vimentin binding to receptor phosphatase β and subsequent polymerization of the phosphatase, which stimulates a cascade of AKT activation and increased cell proliferation (30). In a model of non-alcoholic fatty liver disease and hepatocellular cancer, insulin resistance has also associated with up-regulation of Vimentin, however in that model metastatic disease was not studied (31). Insulin has been shown to stimulate Vimentin in hepatocytes in a model of hepatitis C infection (32). Our current study shows that insulin increases Vimentin expression in breast cancer cells and has an important role in insulin-mediated cell invasion *in vitro* and tumor metastases in the setting of pre-diabetes *in vivo*.

In breast cancer, cancer-associated cells (e.g. fibroblasts, lymphocytes) can express Vimentin (33). In the inducible Her2 model of breast cancer, we previously found that the primary tumors from the hyperinsulinemic mice expressed higher levels of Vimentin compared to the primary tumors from the control mice (34). The immunofluorescent staining of the paraffin embedded tumors showed significantly increased Vimentin expression in the hyperinsulinemic mice compared to the controls (34). Interestingly, the Vimentin positive stains did not stain positive for Her2/Neu so it was not possible to distinguish if the tumor cells had undergone EMT or if these Vimentin positive cells were invading fibroblasts (34). In the current study, we utilized GFP tagged c-Myc/Vegf overexpressing cells to establish which cells were responsible for the Vimentin expression. Utilizing immunofluorescent staining of the paraffin embedded primary tumors we observed a clear co-staining of Vimentin with GFP, elucidating that it is the primary tumor cells which increase the expression of Vimentin in the setting of hyperinsulinemia.

Vimentin null mice do not exhibit any apparent developmental defects and have relatively normal phenotypes except when stressed (35). They do have impaired wound healing at the embryonic and adult stages because of abnormal fibroblasts, due to impaired migration (36, 37). These mice have not been used in published oncology studies. *In vitro* studies have demonstrated that silencing Vimentin reduced the migration and invasion of doxorubicin resistant MCF-7 cells (38). siRNA Vimentin silencing has also been shown to impair the invasiveness of metastatic SW480 colon cancer and MDA-MB-231 breast cancer cell lines (39). The two cell lines migrated much slower in a wound-healing assay and had a significantly decreased adhesion to a collagen matrix (39). Our current data are consistent with a previous study in MDA-MB-231 breast cancer cells, reporting that silencing of AXL (a regulator of Vimentin) leads to decreased lung metastasis after intravenous injection (40). However, there are no previous *in vivo* studies evaluating the importance of Vimentin on breast cancer metastasis in the setting of the metabolic syndrome, obesity or pre-diabetes. As breast cancer metastases are more likely in these metabolic conditions, we believe it is important to develop a greater understanding of why this occurs. Therefore, our studies are

the first to show that shRNA silencing of Vimentin leads to a decrease in pulmonary metastasis from primary tumors *in vivo*, using a c-Myc/Vegf overexpressing breast cancer cell line.

In addition to its association with cells undergoing EMT, Vimentin has also been shown to act as a chaperone-like molecule and bind AKT. In soft tissue sarcoma cells, AKT activation leads to increased cell survival and migration, and associates with phosphorylated forms of Vimentin leading to protection against caspase-induced proteolysis (21). *In vivo*, hyperinsulinemia led to increased AKT phosphorylation in MVT-1 tumors (12), but we found no change in ERK1/2, p38-MAPK, or Wnt signaling in the MVT-1 tumors from the WT and MKR mice (Figure S6). The cleavage of Vimentin was propagated by Caspase 3 (21). The data in the current study show that insulin leads to a decrease in active Caspase 3 levels. The data also show that inhibiting PI3K with NVP-BKM120 leads to an increase in active Caspase 3 levels and a decrease in Vimentin expression. This data support the observation that silencing Vimentin impaired the increased invasion stimulated by insulin. This suggests that Vimentin could potentiate insulin action on breast cancer metastasis.

In summary, we demonstrate using a pre-diabetic, hyperinsulinemic mouse model, that insulin promotes an increased expression of Vimentin in breast tumors, and is associated with an increase in pulmonary metastases. To our knowledge, no previous studies have examined the *in vivo* role of Vimentin in breast cancer metastases in the setting of metabolic conditions, such as obesity, pre-diabetes or diabetes. In addition, these studies are the first to show a protein that can be targeted to reduce metastases in the setting of hyperinsulinemia. We propose that insulin acting through the PI3K/AKT pathway induces the increase of Vimentin expression by blocking Caspase 3 activation. This suggests that in breast cancer patients, with metabolic conditions associated with endogenous hyperinsulinemia, therapies to reduce Vimentin expression or function could play an important role in reducing mortality from breast cancer metastases.

Materials and Methods

Animal Studies

All mouse procedures were in compliance with the standards specified in the Guide of the Care and Use of Laboratory Animals provided by the Association for Assessment and Accreditation of Laboratory Animal Care (AAALAC) and approved by Mount Sinai Institutional Animal Care and Use Committee and are previously described (12). Briefly, at 8 weeks of age, 100,000 MVT-1 cells resuspended in 100μL of sterile PBS were injected into the 4th mammary fat pad. Studies were done in duplicate with n=5, 12 for WT and n= 8, 12 for MKR mice in each study respectively. The number of animals was chosen based off our previous studies that showed significant increase in tumor growth and pulmonary metastasis in MKR mice compared to control. Tumor and lung metastases protocols are described here (12).

Vimentin shRNA

Glycerol stocks of lentiviral shRNA targeting Vimentin were obtained from Sigma-Aldrich (St. Louis, MO). shRNA sequences were: control shRNA: CAACAAGATGAAGAGCACCAA; Vimentin shRNA TRC317673: GCTTCAAGACTCGGTGGACTT; Vimentin shRNA TRC 317676: GCGCAAGATAGATTTGGAATA. The shRNA of the Vimentin targets and control were infected into MVT-1 cells by previously described methods (41, 42), utilizing QIAprep Miniprep and Qiagen Plasmid Maxi Kit to obtain plasmid DNA following the manufacturer's protocol (QIAGEN, Valencia, CA). HEK293FT cells were transfected with 20μg of lentiviral DNA and 10μg of each helper plasmid (gag/pol and env). The virus was concentrated and the target cells were infected in duplicate with lentiviral control or Vimentin shRNA virus. After the infection, 2–3 weeks of 2.5μg/ml puromycin was used for selection for stable knockdown of the target gene. Successful gene and protein knockdown was confirmed by Real Time qPCR and Western Blot analysis. At 8 weeks of age, 100,000 MVT-1 Control or MVT-1 Vimentin Knockdown cells resuspended in 100μL of sterile PBS were injected into the 4^{th} mammary fat pad. Studies were done in duplicate with n=4, 10 WT Control, n=5, 10 for WT Vimentin Knockdown, n=10, 13 for MKR Control, and n=10, 12 for MKR Vimentin Knockdown in each study respectively. Mice were randomized into groups based on body weights before injected with either MVT-1 Control or MVT-1 Vimentin Knockdown cells. There was no blinding of the experiment.

Real Time qPCR

RNA was extracted from cells using the RNeasy Mini Kit (QIAGEN, Valencia, CA) according to the manufacturer's instructions. One μg of RNA was reverse-transcribed to cDNA using oligo (dT) primers with a RT-PCR kit according to the manufacturer's instructions (Invitrogen, Carlsbad, CA). Following reverse transcription, cDNA was subjected to real time-PCR using the QuantiTect SYBR green PCR kit (QIAGEN, Valencia, CA) in ABI PRISM 7900HT sequence detection systems (Applied Biosystems, Foster City, CA). Primer sequences: Vimentin 5′CTGAGGCTGCCAACCGGAACAA, 3′CCTCGCCTTCCAGCAGCTTCC. β-actin 5′CCTAAGGCCAACCGTGAAAA, 3′GAGGCATACAGGGACAGCACA.

Generation of green fluorescent protein–expressing (GFP) cell line

A construct containing GFP (NV-SV-40-puro-linkek-Ins-PGK-eGFP) was received as a gift from Dr. Neufeld, Technion, Haifa, Israel. The sequence was transfected into the Lentiviral packaging cell line HEK293FT together with ViraPower packaging mix (Invitrogen, Carlsbad, CA) by using the Lipofectamine 2000 reagent (Invitrogen, Carlsbad, CA). The virus was concentrated and the target MVT-1 cells were infected. Infected cells were selected and maintained with 2μg/mL puromycin.

Cell Culture

Mouse MVT-1 cells were a donation from K. Hunter at the Center for Cancer Research in the National Institute of Health. The MVT-1 cells were derived from MMTV c-Myc/Vegf transgenic female mice (43). Cells were tested and were negative for all mycoplasma

species. Cells were grown in Dulbecco's Modified Eagles Medium (DMEM) supplemented with 10% Fetal Bovine Serum (FBS) (Invitrogen Life Technologies, Grand Island, NY), 100 U/ml penicillin and 100ug/ml streptomycin (Mediatech, Manassas, VA). For cells with lentiviral plasmid DNA cells were maintained in medium supplemented with 1.5μg/ml puromycin. All cells were grown at 37C in 5% CO2 atmosphere. All cell culture experiments were conducted in triplicate and experiments were repeated three times.

Cell Stimulation and PI3K Inhibition

MVT-1 cells were plated in 10cm plates and allowed to grow to 50% confluency. Standard growth medium was exchanged for serum-free DMEM containing 0.1% Bovine Serum Albumin (BSA) (Sigma-Aldrich, St. Louis, MO), 100 U/ml penicillin and 100ug/ml streptomycin overnight. The cells were incubated with insulin (Lily, Indianapolis, IN) at 10nM concentration or vehicle (PBS with 0.1% BSA) for 48 hours. For PI3K inhibition, MVT-1 cells plated in 10cm plates were pre-treated with 500nM NVP-BKM120, (Novartis Pharmaceuticals, Basel Switzerland), or DMSO for 1hr post overnight serum starvation. The cells were treated with 10nM Insulin or Vehicle in PBS with 0.1% BSA for 48 hours. For all stimulations serum-free DMEM containing 0.1% Bovine Serum Albumin (BSA), 100 U/ml penicillin and 100ug/ml streptomycin was replaced after 24 hours and appropriate agents reintroduced.

Western Blotting

MVT-1 cells and tumor tissue extraction methods are described here (12). The western bands were quantified using open source Image J software (National Institutes of Health, Bethesda, MD).

Immunoprecipitation and Proteomic Analysis

Immunoprecipitation of Vimentin was performed following the manufacturer's protocol using magnetic Dynabeads Protein G (Invitrogen Life Technologies, Grand Island, NY). The protocol was modified by utilizing 1mg of protein lysate with 10μg anti-Vimentin antibody incubated at 4ºC overnight with rotation. Samples were incubated with magnetic beads for 4h at 4ºC with rotation and then washed with ice-cold tris buffer (pH 7.4). Antigen was eluted in 3X loading buffer supplemented with DTT. Samples were denatured at 96ºC for 5min and loaded on an 8% Tris-Glycine gel. Gel was stained in 0.025% Coomassie G-250 blue dye (Amresco, Solon, OH), 10% acetic acid and 50% methanol for 1hr, destained in 10% acetic acid and 50% methanol and stored in ddH2O. The Mount Sinai Proteomics core then analyzed the bands of interest. The Vimentin double band (higher and lower molecular weight) was excised from the gel, reduced with TCEP and alkylated with iodoacetamide and analyzed by mass spectrometry after trypsin digestion. The analysis was performed using reversed-phase liquid chromatography (LC) over a Waters BEH130 C18 column (100 μm × 100 mm, 1.7 μm particle size) in a Waters NanoAcquity UPLC system (Waters, Milford, MA) interfaced to a Thermo LTQ-Orbitrap mass spectrometer (Thermo Scientific, San Jose, CA).

Antibodies

The Western Blot nitrocellulose membranes were probed with the following primary antibodies: anti-Vimentin (Catalog:5741), anti-phospho Akt $^{(Ser473)}$ (Catalog:9271), anti-total Akt (Catalog:2920), Caspase 3 (Catalog:9662), PARP (Catalog:9542) (Cell Signaling Technology, Danvers, MA), anti-Vimentin (Catalog:SC-373717) (Santa Cruz Biotechnology, Dallas, TX), and anti-β-actin (Catalog:A1978) (Sigma-Aldrich, St. Louis, MO).

For immunoprecipitation, the mouse monoclonal anti-Vimentin (Catalog:SC-373717) (Santa Cruz Biotechnology, Dallas, TX) was used.

Immunofluorescence

Primary mammary tumors were cut at the time of sacrifice, fixed in 10% formalin, transferred to 70% ethanol, embedded in paraffin, and sectioned at 5micron. The sections were deparaffinized, rehydrated and subjected to antigen retrieval as previously described (44). Primary antibodies anti-Vimentin (Cell Signaling, Danvers, MA) and secondary AlexaFluor568-conjugated (red) donkey antirabbit IgG (1:500, Molecular Probes, Eugene, OR) and AlexaFluor488-conjugated (green) goat antimouse IgG (1:500; Molecular Probes) for 2h were used. Nuclei were counterstained with 0.2μg/ml 4′,6-diamidino-2-phenylindole (DAPI; Sigma–Aldrich, St. Louis, MO). Sections were mounted using Fluorogel mounting medium (Electron Microscopy Sciences, Hatfield, PA). An Olympus AX70 fluorescence microscope (Olympus, Center Valley, PA) was used to capture images from immunofluorescence staining with CellSens software (Olympus, Center Valley, PA) software. At least six individual ×400 fields per group were captured for counting Vimentin-positive cells and the total number of DAPI-positive cells. Quantification of the intensity of the Vimentin-positive cells was performed using CellSens Software (Olympus, Center Valley, PA).

Proliferation, Migration and Invasion Assays

For the proliferation assay, Cell Counting Kit-8 (CCK-8) was used (Dojindo Molecular Technologies Inc, Rockville, MD). Cell number to OD curve was generated for the MVT-1 control and Vimentin knockdown cells per the manufacturer's protocol, no significant difference was observed between the two cell lines. 5,000 MVT-1 control and 5,000 MVT-1 Vimentin knockdown cells were plated in 96-well plates in phenol free DMEM with 10% FBS, 100 U/ml penicillin and 100μg/ml streptomycin ("Complete Medium"). The cells analyzed for cell proliferation at 24, 48, and 72h, taking the absorbance readings 3 hours after the addition of CCK-8 reagent.

For the migration assay, transwell permeable inserts with 8μm sized-pores were used (Corning Inc, Corning, NY). 500μL of Complete Media was added to the lower chamber. 150,000 MVT-1 cells (control or Vimentin shRNA knockdown) were seeded in 300μl of Complete Media in the insert. For the invasion assay, 24 well Corning BioCoat Tumor Invasion System with 8μm pore inserts was used. Similar to the migration assay, 500μL of Complete Media or when appropriate 0.1% BSA (with or without 10nM insulin) was added to the lower chamber. The insert was seeded with 400,000 MVT-1 cells (control or Vimentin knockdown) in 300μl of Complete Media. For the insulin stimulation studies, the standard

DMEM was exchanged for serum-free DMEM contained 0.1% BSA, 100 U/ml penicillin and 100μg/ml streptomycin. 400,000 MVT-1 control and knockdown cells treated with 10nM insulin diluted in PBS with 0.1% BSA or vehicle. For both the migration and invasion assays, the number of cells migrated and invaded was analyzed as previously described (45), with the modification of measuring the optical density of the eluted crystal violet dye at 595nm on a plate spectrophotometer. For both the migration and invasion assays, cell number was extrapolated by performing serial dilutions from 64,000 to 250 cells in a 96-well plate following previously described methods (45). The OD versus cell number standard curve was generated.

Statistical analysis

All data expressed as mean ± standard error of the mean (SEM). Student's t-test and two-way ANOVA followed by Tukey HSD post-hoc test, was used with P value ≤ 0.05 considered statistically significant using GraphPad Prism Software (La Jolla, CA). The Shapiro Wilk Test for normality was used and for groups that were not normally distributed, a non-parametric test (Kruskal Wallis Test) was performed. F-test was performed to check for variance and there was equal variance between groups being statistically compared.

Supplementary Material

Refer to Web version on PubMed Central for supplementary material.

Acknowledgments

Financial Support: NCI grant (Grant 2R01CA128799-06A1) to DLR. American Diabetes grant 1-13-BS-108 to DLR. NIH/NCI 1K08CA190770 to EJG. NCI Supplement R01CA171558-02S1 to YD. Scuola di Specializzazione in Endocrinologia e Malattie del Metabolismo, University of Pisa to VB.

References

1. Redaniel MT, Jeffreys M, May MT, Ben-Shlomo Y, Martin RM. Associations of type 2 diabetes and diabetes treatment with breast cancer risk and mortality: a population-based cohort study among British women. Cancer causes & control : CCC. 2012; 23(11):1785–95. Epub 2012/09/14. [PubMed: 22971998]
2. Yang Y, Mauldin PD, Ebeling M, Hulsey TC, Liu B, Thomas MB, et al. Effect of metabolic syndrome and its components on recurrence and survival in colon cancer patients. Cancer. 2012 Epub 2013/01/03.
3. Zanders MM, Boll D, van Steenbergen LN, van de Poll-Franse LV, Haak HR. Effect of diabetes on endometrial cancer recurrence and survival. Maturitas. 2013; 74(1):37–43. Epub 2012/11/17. [PubMed: 23153683]
4. Lawlor DA, Smith GD, Ebrahim S. Hyperinsulinaemia and increased risk of breast cancer: findings from the British Women's Heart and Health Study. Cancer causes & control : CCC. 2004; 15(3): 267–75. Epub 2004/04/20. [PubMed: 15090721]
5. Ouchi N, Parker JL, Lugus JJ, Walsh K. Adipokines in inflammation and metabolic disease. Nature reviews Immunology. 2011; 11(2):85–97. Epub 2011/01/22.3518031.
6. Goodwin PJ, Ennis M, Pritchard KI, Trudeau ME, Koo J, Madarnas Y, et al. Fasting insulin and outcome in early-stage breast cancer: results of a prospective cohort study. Journal of clinical oncology : official journal of the American Society of Clinical Oncology. 2002; 20(1):42–51. Epub 2002/01/05. [PubMed: 11773152]

7. Lipscombe LL, Goodwin PJ, Zinman B, McLaughlin JR, Hux JE. The impact of diabetes on survival following breast cancer. Breast cancer research and treatment. 2008; 109(2):389–95. Epub 2007/07/31. [PubMed: 17659440]
8. DeFronzo RA. Pathogenesis of type 2 diabetes mellitus. The Medical clinics of North America. 2004; 88(4):787–835. ix. Epub 2004/08/17. [PubMed: 15308380]
9. LeRoith D, Gavrilova O. Mouse models created to study the pathophysiology of Type 2 diabetes. The international journal of biochemistry & cell biology. 2006; 38(5–6):904–12. Epub 2005/08/17. [PubMed: 16103004]
10. Fernandez AM, Kim JK, Yakar S, Dupont J, Hernandez-Sanchez C, Castle AL, et al. Functional inactivation of the IGF-I and insulin receptors in skeletal muscle causes type 2 diabetes. Genes & development. 2001; 15(15):1926–34. Epub 2001/08/04.312754. [PubMed: 11485987]
11. Novosyadlyy R, Lann DE, Vijayakumar A, Rowzee A, Lazzarino DA, Fierz Y, et al. Insulin-mediated acceleration of breast cancer development and progression in a nonobese model of type 2 diabetes. Cancer research. 2010; 70(2):741–51. Epub 2010/01/14.2946167. [PubMed: 20068149]
12. Ferguson RD, Novosyadlyy R, Fierz Y, Alikhani N, Sun H, Yakar S, et al. Hyperinsulinemia enhances c-Myc-mediated mammary tumor development and advances metastatic progression to the lung in a mouse model of type 2 diabetes. Breast cancer research : BCR. 2012; 14(1):R8. Epub 2012/01/10.3496123. [PubMed: 22226054]
13. Franke WW, Grund C, Kuhn C, Jackson BW, Illmensee K. Formation of cytoskeletal elements during mouse embryogenesis. III. Primary mesenchymal cells and the first appearance of vimentin filaments. Differentiation; research in biological diversity. 1982; 23(1):43–59. Epub 1982/01/01. [PubMed: 6759279]
14. Thiery JP. Epithelial-mesenchymal transitions in tumour progression. Nature reviews Cancer. 2002; 2(6):442–54. Epub 2002/08/22. [PubMed: 12189386]
15. Mendez MG, Kojima S, Goldman RD. Vimentin induces changes in cell shape, motility, and adhesion during the epithelial to mesenchymal transition. FASEB journal : official publication of the Federation of American Societies for Experimental Biology. 2010; 24(6):1838–51. Epub 2010/01/26.2874471. [PubMed: 20097873]
16. Wei J, Xu G, Wu M, Zhang Y, Li Q, Liu P, et al. Overexpression of vimentin contributes to prostate cancer invasion and metastasis via src regulation. Anticancer research. 2008; 28(1A):327–34. Epub 2008/04/04. [PubMed: 18383865]
17. Fierz Y, Novosyadlyy R, Vijayakumar A, Yakar S, LeRoith D. Insulin-sensitizing therapy attenuates type 2 diabetes-mediated mammary tumor progression. Diabetes. 2010; 59(3):686–93. Epub 2009/12/05.2828655. [PubMed: 19959755]
18. Rostoker R, Abelson S, Bitton-Worms K, Genkin I, Ben-Shmuel S, Dakwar M, et al. Highly specific role of the insulin receptor in breast cancer progression. Endocrine-related cancer. 2015; 22(2):145–57. Epub 2015/02/20.4362669. [PubMed: 25694511]
19. Borowsky AD, Namba R, Young LJ, Hunter KW, Hodgson JG, Tepper CG, et al. Syngeneic mouse mammary carcinoma cell lines: two closely related cell lines with divergent metastatic behavior. Clinical & experimental metastasis. 2005; 22(1):47–59. Epub 2005/09/01. [PubMed: 16132578]
20. Samani AA, Yakar S, LeRoith D, Brodt P. The role of the IGF system in cancer growth and metastasis: overview and recent insights. Endocrine reviews. 2007; 28(1):20–47. Epub 2006/08/26. [PubMed: 16931767]
21. Zhu QS, Rosenblatt K, Huang KL, Lahat G, Brobey R, Bolshakov S, et al. Vimentin is a novel AKT1 target mediating motility and invasion. Oncogene. 2011; 30(4):457–70. Epub 2010/09/22.3010301. [PubMed: 20856200]
22. Los M, Mozoluk M, Ferrari D, Stepczynska A, Stroh C, Renz A, et al. Activation and caspase-mediated inhibition of PARP: a molecular switch between fibroblast necrosis and apoptosis in death receptor signaling. Molecular biology of the cell. 2002; 13(3):978–88. Epub 2002/03/22.99613. [PubMed: 11907276]
23. Adami HO, McLaughlin J, Ekbom A, Berne C, Silverman D, Hacker D, et al. Cancer risk in patients with diabetes mellitus. Cancer causes & control : CCC. 1991; 2(5):307–14. Epub 1991/09/01. [PubMed: 1932543]

24. Chari ST, Leibson CL, Rabe KG, Ransom J, de Andrade M, Petersen GM. Probability of pancreatic cancer following diabetes: a population-based study. Gastroenterology. 2005; 129(2): 504–11. Epub 2005/08/09.2377196. [PubMed: 16083707]
25. Onitilo AA, Engel JM, Glurich I, Stankowski RV, Williams GM, Doi SA. Diabetes and cancer I: risk, survival, and implications for screening. Cancer causes & control : CCC. 2012; 23(6):967–81. Epub 2012/05/04. [PubMed: 22552844]
26. Zhang PH, Chen ZW, Lv D, Xu YY, Gu WL, Zhang XH, et al. Increased risk of cancer in patients with type 2 diabetes mellitus: A retrospective cohort study in China. BMC public health. 2012; 12(1):567. Epub 2012/07/31. [PubMed: 22839452]
27. Haslam DW, James WP. Obesity. Lancet. 2005; 366(9492):1197–209. Epub 2005/10/04. [PubMed: 16198769]
28. Gilles C, Polette M, Zahm JM, Tournier JM, Volders L, Foidart JM, et al. Vimentin contributes to human mammary epithelial cell migration. Journal of cell science. 1999; 112(Pt 24):4615–25. Epub 1999/11/27. [PubMed: 10574710]
29. Satelli A, Li S. Vimentin in cancer and its potential as a molecular target for cancer therapy. Cellular and molecular life sciences : CMLS. 2011; 68(18):3033–46. Epub 2011/06/04.3162105. [PubMed: 21637948]
30. Shen X, Xi G, Wai C, Clemmons DR. The Coordinate Cellular Response to Insulin-like Growth Factor-I (IGF-I) and Insulin-like Growth Factor-binding Protein-2 (IGFBP-2) Is Regulated through Vimentin Binding to Receptor Tyrosine Phosphatase beta (RPTPbeta). The Journal of biological chemistry. 2015; 290(18):11578–90. Epub 2015/03/20.4416861. [PubMed: 25787077]
31. Hines IN, Hartwell HJ, Feng Y, Theve EJ, Hall GA, Hashway S, et al. Insulin resistance and metabolic hepatocarcinogenesis with parent-of-origin effects in AxB mice. The American journal of pathology. 2011; 179(6):2855–65. Epub 2011/10/05.3260805. [PubMed: 21967816]
32. Svegliati-Baroni G, Faraci G, Fabris L, Saccomanno S, Cadamuro M, Pierantonelli I, et al. Insulin resistance and necroinflammation drives ductular reaction and epithelial-mesenchymal transition in chronic hepatitis C. Gut. 2011; 60(1):108–15. Epub 2010/10/23.3784835. [PubMed: 20966027]
33. Yu Y, Xiao CH, Tan LD, Wang QS, Li XQ, Feng YM. Cancer-associated fibroblasts induce epithelial-mesenchymal transition of breast cancer cells through paracrine TGF-beta signalling. British journal of cancer. 2014; 110(3):724–32. Epub 2013/12/18.3915130. [PubMed: 24335925]
34. Ferguson RD, Gallagher EJ, Cohen D, Tobin-Hess A, Alikhani N, Novosyadlyy R, et al. Hyperinsulinemia promotes metastasis to the lung in a mouse model of Her2-mediated breast cancer. Endocrine-related cancer. 2013; 20(3):391–401. Epub 2013/04/11. [PubMed: 23572162]
35. Colucci-Guyon E, Portier MM, Dunia I, Paulin D, Pournin S, Babinet C. Mice lacking vimentin develop and reproduce without an obvious phenotype. Cell. 1994; 79(4):679–94. Epub 1994/11/18. [PubMed: 7954832]
36. Eckes B, Colucci-Guyon E, Smola H, Nodder S, Babinet C, Krieg T, et al. Impaired wound healing in embryonic and adult mice lacking vimentin. Journal of cell science. 2000; 113(Pt 13):2455–62. Epub 2000/06/15. [PubMed: 10852824]
37. Eckes B, Dogic D, Colucci-Guyon E, Wang N, Maniotis A, Ingber D, et al. Impaired mechanical stability, migration and contractile capacity in vimentin-deficient fibroblasts. Journal of cell science. 1998; 111(Pt 13):1897–907. Epub 1998/06/17. [PubMed: 9625752]
38. Tezcan O, Gunduz U. Vimentin silencing effect on invasive and migration characteristics of doxorubicin resistant MCF-7 cells. Biomedicine & pharmacotherapy = Biomedecine & pharmacotherapie. 2014; 68(3):357–64. Epub 2014/03/13. [PubMed: 24612689]
39. McInroy L, Maatta A. Down-regulation of vimentin expression inhibits carcinoma cell migration and adhesion. Biochemical and biophysical research communications. 2007; 360(1):109–14. Epub 2007/06/26. [PubMed: 17585878]
40. Vuoriluoto K, Haugen H, Kiviluoto S, Mpindi JP, Nevo J, Gjerdrum C, et al. Vimentin regulates EMT induction by Slug and oncogenic H-Ras and migration by governing Axl expression in breast cancer. Oncogene. 2011; 30(12):1436–48. Epub 2010/11/09. [PubMed: 21057535]
41. Moore CB, Guthrie EH, Huang MT, Taxman DJ. Short hairpin RNA (shRNA): design, delivery, and assessment of gene knockdown. Methods Mol Biol. 2010; 629:141–58. Epub 2010/04/14.3679364. [PubMed: 20387148]

42. Beronja S, Livshits G, Williams S, Fuchs E. Rapid functional dissection of genetic networks via tissue-specific transduction and RNAi in mouse embryos. Nature medicine. 2010; 16(7):821–7. Epub 2010/06/08.2911018.

43. Pei XF, Noble MS, Davoli MA, Rosfjord E, Tilli MT, Furth PA, et al. Explant-cell culture of primary mammary tumors from MMTV-c-Myc transgenic mice. In vitro cellular & developmental biology Animal. 2004; 40(1–2):14–21. Epub 2004/06/08. [PubMed: 15180438]

44. Cannata D, Lann D, Wu Y, Elis S, Sun H, Yakar S, et al. Elevated circulating IGF-I promotes mammary gland development and proliferation. Endocrinology. 2010; 151(12):5751–61. Epub 2010/10/12.2999497. [PubMed: 20926579]

45. Marshall J. Transwell((R)) invasion assays. Methods Mol Biol. 2011; 769:97–110. Epub 2011/07/13. [PubMed: 21748672]

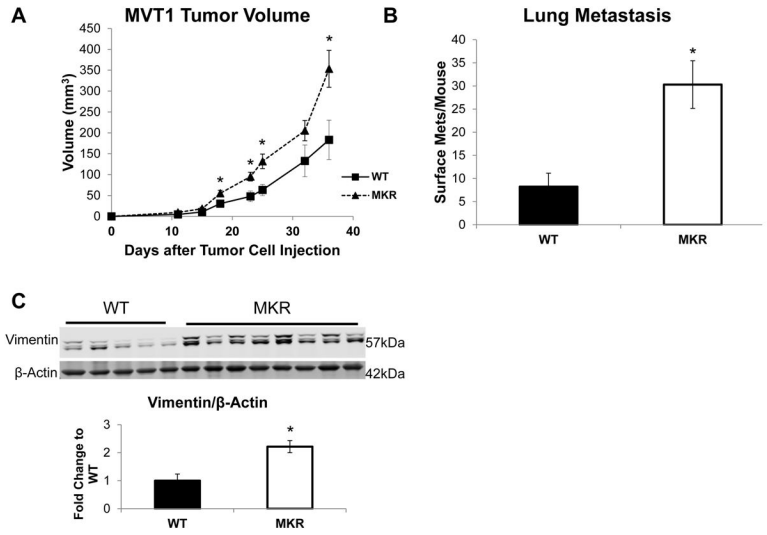

Figure 1.

Tumors from hyperinsulinemic mice have increased Vimentin protein expression. Wild type (WT) and hyperinsulinemic (MKR) were injected with MVT-1 cells (c-Myc/Vegf overexpressing cell line) into the 4th mammary fat pad (5–12 mice per group). (A.) Mammary tumor volume was measured twice weekly with calipers. (B.) Number of surface pulmonary macrometastases in both WT and MKR mice. (C.) Representative blots showing protein extracted from tumor tissue and analyzed by Western blot for Vimentin expression (both bands). β-Actin antibody used as loading control. (D.) Densitometry of western blot (* $p<0.05$). All graphs represent mean per group and error bars are SEM.

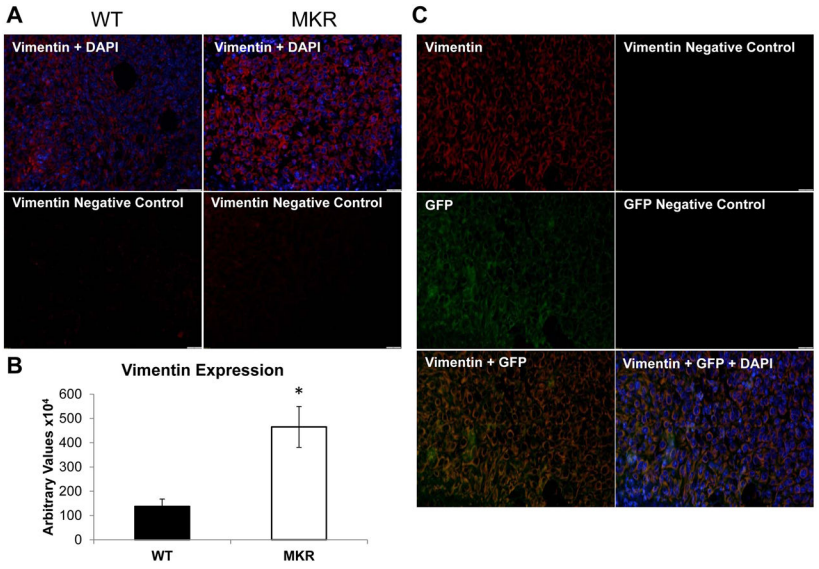

Figure 2.

Vimentin expression is enhanced in tumors from MKR mice compared to WT controls. (A.) Tumor sections from wild type and MKR mice analyzed by immunofluorescence for Vimentin (red) expression. Nuclei stained with DAPI (blue). (B.) Quantification of Vimentin expression n=5 per group, with 6 sections per tumor. * $p<0.05$. Graphs represent mean per group and error bars are SEM. (C.) MVT-1 cells were GFP tagged and injected into wild type and MKR mice. Representative tumor sections show co-expression Vimentin and GFP by immunofluorescence. Nuclei were stained with DAPI (blue).

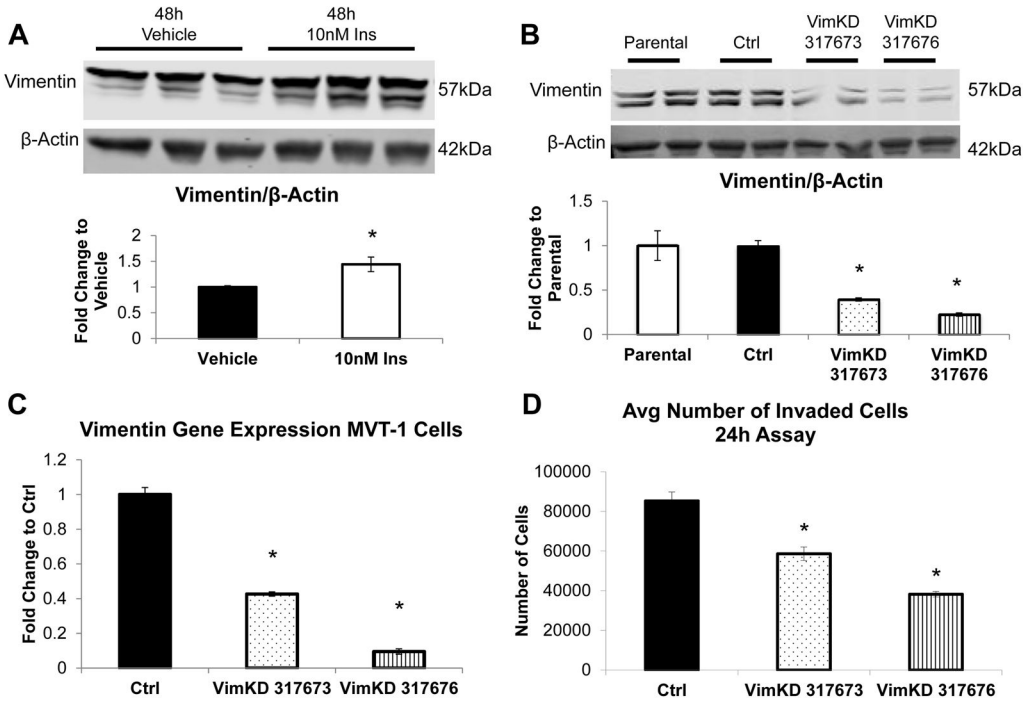

Figure 3.

Knockdown (KD) of Vimentin expression in MVT-1 cells. (A) Analysis of Vimentin protein expression from MVT-1 cells stimulated with 10nM insulin (n=3) or PBS control (n=3) for 48 hours, repeated 4 times. β-Actin was used as a loading control. Representative western blot of experiments. Densitometry of western blot from 4 experiments (* $p<0.05$). (B.) Lentiviral shRNA for Vimentin and control sequence was used to generate MVT-1 cells with a knockdown of Vimentin protein expression. Cells were grown, protein was harvested and protein lysates were run to analyze two different clones for Vimentin KD. Densitometry analysis of Vimentin protein expression (both bands) of the parental, control, Vimentin 317673 clone, and Vimentin 317676 clone (n=2, repeated 3 times). (C.) mRNA was extracted and gene expression levels were analyzed using quantitative Real Time PCR. (D.) 400,000 MVT-1 Control, Vimentin 317673 clone, and Vimentin 317676 clone cells were plated into 0.8μm inserts coated with matrigel in Complete Medium. The number of cells that invaded through the matrigel coated insert after 24 hours was quantified by crystal violet staining, repeated 3 times. * $p<0.05$. All graphs represent mean per group and error bars are SEM.

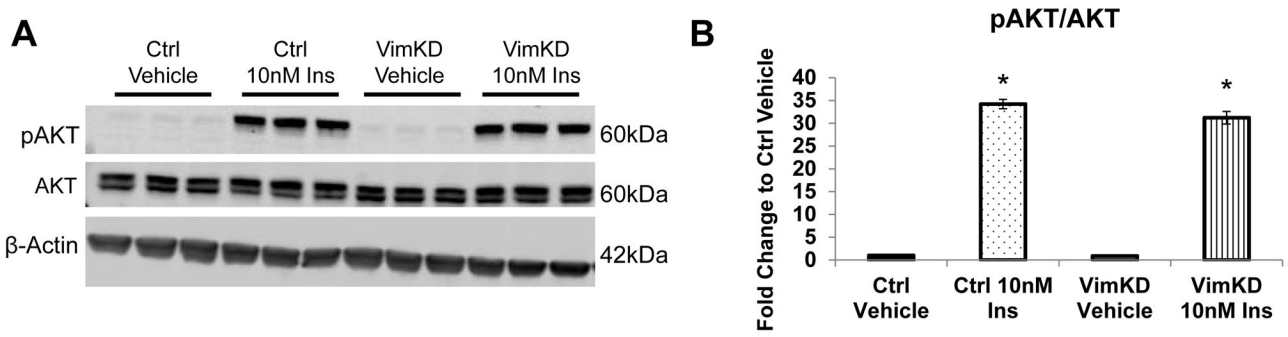

Figure 4.

Insulin Signaling preserved in Vimentin Knockdown Cells. (A.) Cells were serum starved overnight and stimulated with 10nM insulin (Ins) for 15 min. Protein was extracted from the cells and analyzed by Western blotting. (n=3 per condition, repeated two times) (B.) Densitometry of pAKT/AKT. * $p<0.05$. Graphs represent mean per group and error bars are SEM.

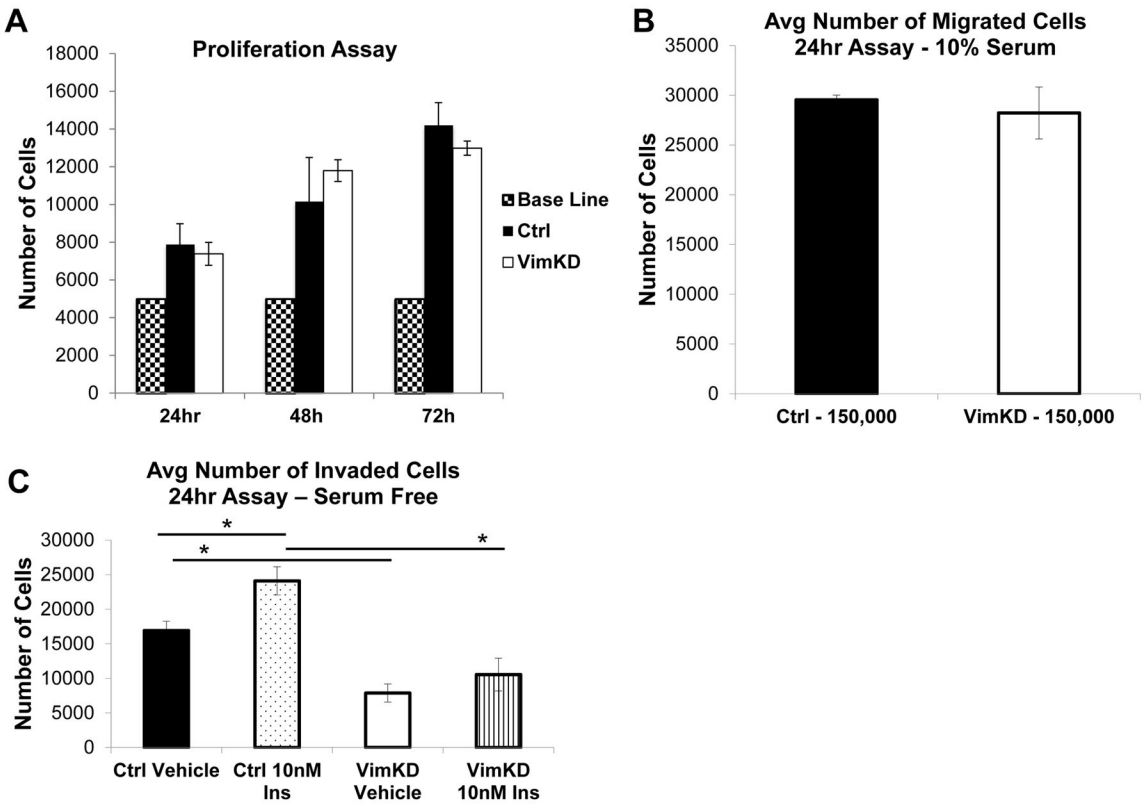

Figure 5.

Silencing Vimentin decreased cell invasion but not proliferation or migration. (A.) Cell counting kit 8 (CCK-8) was used for determination of cell proliferation between MVT-1 control (Ctrl) and MVT-1 Vimentin knockdown (VimKD) cells. 5,000 cells were plated in Complete Medium an analyzed for cell proliferation at 24, 48 and 72 hours, repeated twice. (B.) 150,000 MVT-1 Ctrl and MVT-1 VimKD cells were plated in 0.8μm inserts. The number of cells that migrated through the insert after 24 hours in Complete Medium was quantified by crystal violet staining, repeated three times. (C.) 400,000 MVT-1 Ctrl and MVT-1 VimKD cells were plated into 0.8μm inserts coated with matrigel. Cells were stimulated with PBS or 10nM Insulin for 24hours in Serum Free Medium. The number of cells that invaded through the matrigel-coated insert after 24 hours was quantified by crystal violet staining, repeated 3 times.

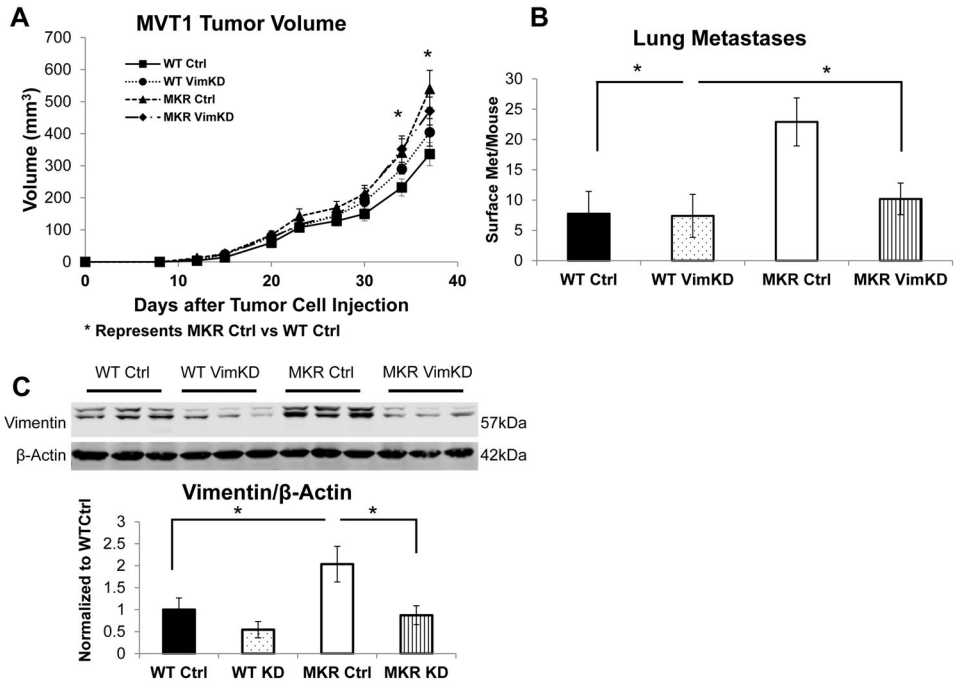

Figure 6.

Knockdown of Vimentin leads to decreased number of pulmonary metastases in the hyperinsulinemic mice. Wild type (10 per group) and MKR (13 per group) mice were injected with 100,000 of MVT-1 Control (Ctrl) and 100,000 of MVT-1 Vimentin KD (VimKD) into the 4th mammary fat pad. (A.) Tumor volumes were measured with calipers. Significant difference between the tumor sizes of MKR Ctrl and WT Ctrl group was observed. * $p<0.05$. (B.) Numbers of surface pulmonary macrometastases in WT and MKR mice. * $p<0.05$, as indicated. (C.) Tumor tissue was extracted and analyzed for Western Blot for Vimentin antibody. Representative blot is shown. Densitometry of Vimentin of representative blot n=3 WT Ctrl, n=4 WT VimKD, n=3 MKR Ctrl, and n=4 MKR VimKD. β-Actin antibody used as a loading control. Graphs represent mean per group and error bars are SEM.

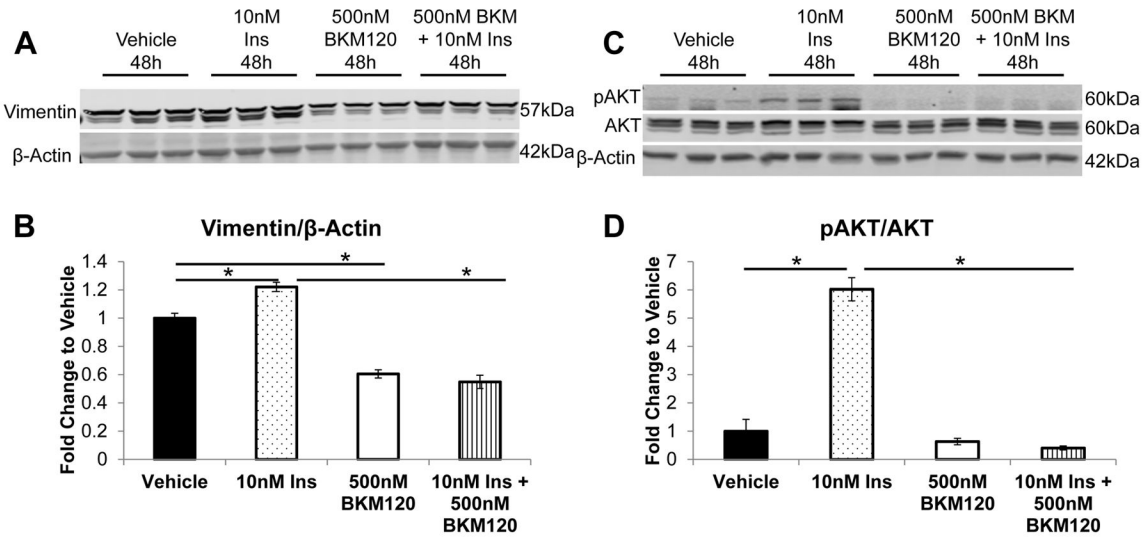

Figure 7.

Inhibition of PI3K/AKT signaling downregulates Vimentin expression. Analysis of the effects of a PI3K inhibitor on the expression of Vimentin was analyzed. MVT-1 cells were serum starved overnight and pretreated for 1 hour with either vehicle or 500nM of NVP-BKM120 (BKM120). Subsequently, cells were stimulated with 10nM of insulin for 48 hours (n=3 per condition, repeated 3 times). Protein was extracted from the cells and analyzed by Western blotting for (A) Vimentin expression and for (B) phosphorylated AKT and total AKT. β-Actin was used as a loading control. (B, D) Densitometry of western blots A and C, respectively (* $p<0.05$). Graphs represent mean per group and error bars are SEM.

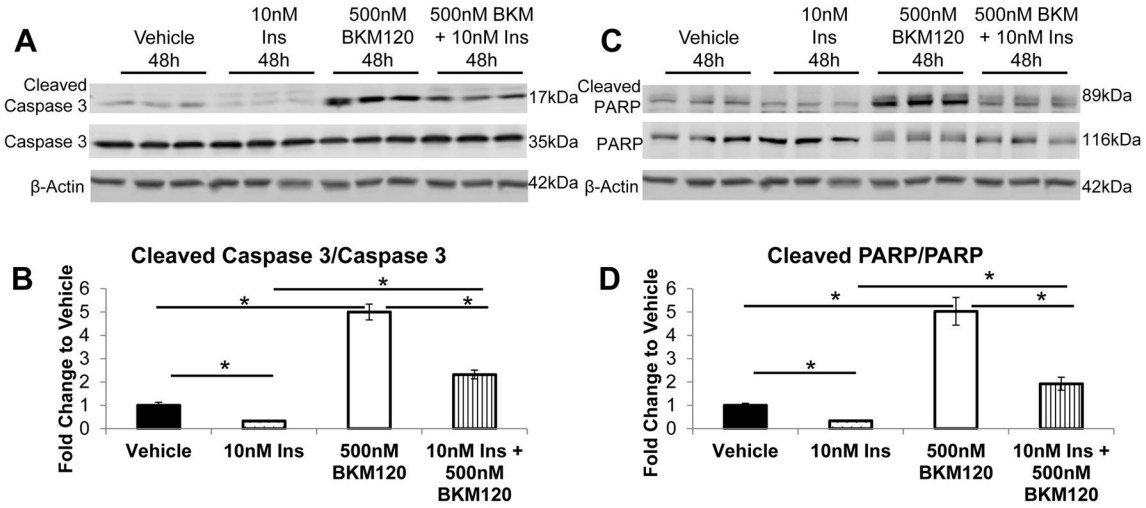

Figure 8.

Insulin prevents the activation of Caspase 3. MVT-1 cells were serum starved overnight and pretreated for 1 hour with either vehicle or 500nM of NVP-BKM120 (BKM120). Subsequently, cells were stimulated with 10nM of insulin for 48 hours (n=3 per condition, repeated 3 times). (A.) Western blotting for cleaved Caspase 3 and total Caspase 3 expression. (B.) Densitometry of cleaved Caspase 3/total Capsase 3 western blot (* $p<0.05$). (C.) Western blotting for cleaved PARP and total PARP expression. (D.) Densitometry of cleaved PARP/total PARP western blot (* $p<0.05$). β-Actin was used as a loading control. All graphs represent mean per group and error bars are SEM.